and S. G. Cohen, *J. Am. Chem. Soc.*, **96**, 2948 (1974); (d) R. O. Loutfy and R. O. Loutfy, *Can. J. Chem.*, **50**, 4052 (1972); (e) J.-P. Bianchi and A. R. Watkins, *J. Chem. Soc., Chem. Commun.*, 265 (1974); (f) P. J. Wagner, A. E. Kamppainen, and T. Jellinek, *J. Am. Chem. Soc.*, **94**, 7512 (1972); (g) J. C. Dalton and J. J. Snyder, *ibid.*, **97**, 5192 (1975).

(15) The observed bimolecular rate constants for fluorescence quenching, k_b^s, given in Table II can also be considered to be the product of k_{diff}, the bimolecular rate constant for formation of an encounter complex, and $k_r/(k_r + k_{-diff})$, the probability that formation of the encounter complex results in quenching (k_r) rather than diffusion apart to regenerate ^{1}A and B (k_{-diff}).[14b,g,16] We assume that k_{diff} and k_{-diff} do not vary with aldehyde structure, since the related rate constants for amine quenching of alkanone fluorescence do not appear to vary with alkanone or amine structure. Under these conditions, variations in k_b^s reflect changes in k_r. See ref 14g for a more detailed discussion.

(16) See, for example, T. R. Evans, *J. Am. Chem. Soc.*, **93**, 2081 (1971).

(17) The bimolecular rate constant for diffusion in hexane has been recently estimated to be 2.9×10^{10} M^{-1} sec^{-1}: P. J. Wagner and I. Kochevar, *J. Am. Chem. Soc.*, **90**, 2232 (1968).

(18) For example, the reduction potentials for acetone and acetaldehyde are −2.3 and −2.1 V, respectively.[14d]

(19) (a) D. Rehm and A. Weller, *Isr. J. Chem.*, **8**, 259 (1970); (b) H. Knibbe, D. Rehm, and A. Weller, *Ber. Bunsenges. Phys. Chem.*, **73**, 839 (1969).

(20) Equation 4 calculates the ΔF values for formation of a charge-transfer complex in which there is full electron transfer from the donor (D) to the acceptor (A). The equation has, however, been usefully applied in cases where charge-transfer complexes are formed with only partial electron transfer.[14] In particular, although the slopes of plots of the log of the bimolecular rate constants for charge-transfer quenching (k_q) of excited states by electron donors vs. the calculated ΔF values vary with the extent of electron transfer in the complex, the k_q values appear to level off when $E(D|D^+) - (E(A^-|A) + \Delta E_{0,0})$ is less than −5 kcal/mol irrespective of the extent of electron transfer.[14a,d,19]

(21) It is difficult to determine the exact difference in alkanal and alkanone ^{1}n,π^* state reduction potentials as defined in eq 4 ($E(A^-|A) + \Delta E_{0,0}$) because the excited singlet state energies, $\Delta E_{0,0}$, are not precisely known. The ground state reduction potentials for model compounds ($E(A^-|A)$ for acetone = −2.3 V; $E(A^-|A)$ for acetaldehyde = −2.1 V)[14d] indicate that if the $\Delta E_{0,0}$ values are comparable, the ^{1}n,π^* state reduction potential will be around 5 kcal/mol greater for alkanals than alkanones. λ_{max} for $S_0 \rightarrow {}^1$n,π^* transitions is generally at somewhat longer wavelength for alkanals than alkanones (ref 12f, p 368–377) suggesting lower $\Delta E_{0,0}$ values for alkanals. On the other hand, we observe that λ_{max} for ^{1}n,$\pi^* \rightarrow S_0$ fluorescence transitions is generally at slightly shorter wavelengths for alkanals than alkanones, suggesting higher $\Delta E_{0,0}$ values for alkanals.

(22) $E(D|D^+)$ for TEA is 22.1 kcal/mol,[14d] $E(A^-|A)$ for acetone is −53.2 kcal/mol,[14d] and $\Delta E_{0,0}$ for the acetone ^{1}n,π^* state is approximately 85 kcal/mol.

(23) The bimolecular rate constant for diffusion in acetonitrile has been estimated to be 2.7×10^{10} M^{-1} sec^{-1} (S. L. Murov, "Handbook of Photochemistry", Marcel Dekker, New York, N.Y., 1973, p 55).

(24) The k_q value given for *t*-DCE quenching of acetone S_1 states is obtained using a τ_f value of 1.7 nsec rather than the value of 2.0 nsec used in ref 5a.

(25) For example, the oxidation potentials of acetone and acetaldehyde are 2.59 and 3.03 V, respectively (R. O. Loutfy and R. O. Loutfy, *J. Phys. Chem.*, **77**, 336 (1973)).

(26) (a) N. J. Turro, *Pure Appl. Chem.*, **27**, 679 (1971); (b) N. J. Turro, C. Lee, N. Schore, J. Barltrop, and H. A. J. Carless, *J. Am. Chem. Soc.*, **93**, 3079 (1971); (c) M. P. Niemczyk, N. E. Schore, and N. J. Turro, *Mol. Photochem.*, **5**, 69 (1973).

(27) Reference 5a reports no quenching of biacetyl fluorescence in benzene with *t*-DCE concentrations greater than 0.1 *M*. Given a τ_f value of 10 nsec for biacetyl in benzene[28] and assuming that at most 10% quenching would go undetected yields 1×10^8 M^{-1} sec^{-1} as a limiting value of k_b^s for *t*-DCE quenching of biacetyl singlets.

(28) N. J. Turro and R. Engel, *J. Am. Chem. Soc.*, **90**, 2989 (1968).

(29) The $\Delta E_{0,0}$ values for the ^{1}n,π^* states of biacetyl and acetone are 65[30] and 85 kcal/mol, respectively, while $E(D|D^+)$ is 60 kcal/mol for acetone and 57 kcal/mol for biacetyl.[31]

(30) S. P. McGlynn, T. Azumi, and M. Kinoshita, "Molecular Spectroscopy of the Triplet State", Prentice-Hall, Englewood Cliffs, N.J., 1969, p 84.

(31) Calculated from the biacetyl ionization potential (IP = 9.57 V)[32] using the following formula: $E(D|D^+) = 0.89\text{IP} - 6.04$.[33]

(32) J. Kelder, H. Cerfontain, B. R. Higginson, and D. R. Lloyd, *Tetrahedron Lett.*, 739 (1974).

(33) L. L. Miller, G. D. Nordblom, and E. A. Mayed, *J. Org. Chem.*, **37**, 916 (1972).

(34) The difference in alkanal and alkanone excited singlet state energies, although not precisely known,[21] is surely less than the 10 kcal/mol difference in alkanal and alkanone oxidation potentials.[25]

(35) For a discussion of single photon counting techniques, see J. B. Birks and J. H. Munro, *Prog. React. Kinet.*, **4**, 215 (1967).

(36) L. Hundley, T. Coburn, E. Garwin, and L. Stryer, *Rev. Sci. Instrum.*, **38**, 488 (1967).

Electronic Structure of Dicarbonyls. Glyoxal Excited States[1]

Clifford E. Dykstra[2] and Henry F. Schaefer III*

Contribution from the Department of Chemistry and Lawrence Berkeley Laboratory, University of California, Berkeley, California 94720. *Received May 8, 1975*

Abstract: Excited electronic states of glyoxal, $(CHO)_2$, have been studied by ab initio self-consistent field (SCF) methods using a double ζ basis set of contracted Gaussian functions. The vertical excitation energies from the optimum ground state geometry were determined for 20 trans and 20 cis excited states. These included all singlet and triplet n → π^* and $\pi \rightarrow \pi^*$ excitations and the lowest n → σ^* excitations. Geometry optimization was performed for the three lowest cis and trans states. Two very low-lying unobserved triplet states, trans ^3B_u and cis $^3B_2$, are predicted by these calculations to be within about 15 000 cm^{-1} of the corresponding ground states, making them possibly the lowest excited states of glyoxal. The next lowest lying states were the observed trans ^3A_u, ^1A_u and cis $^1B_1$, for which the geometry optimization provides a basis for comparison with experiment. The experimentally observed states arise from an n → π^* excitation, but surprisingly the lowest triplets arise from $\pi \rightarrow \pi^*$ excitations. The geometry of these $\pi \rightarrow \pi^*$ triplets is strikingly different from that of the ground state and is in closer correspondence with a biradical structure.

While many excited states of carbon monoxide, formaldehyde, and other carbonyl molecules have been identified,[3a] fewer states of the simplest dicarbonyl, glyoxal, have been observed. Brand identified the first excited states of *trans*-glyoxal as ^1A_u and ^3A_u from his vibrational analysis of the 4550-Å absorption band.[3b] Following the description of McMurry,[3c] these states were associated with an n(a_g) → π^*(a_u) excitation. Extensive high-resolution spectroscopic studies have been made by Ramsay and coworkers.[4-6] In addition, they made the first observation of the cis form of glyoxal and identified the $^1B_1$ excited state in rotational analysis of a band at 4875 Å.[7-9] This state is associated with an n(a_1) → π^*(b_1) excitation and a $^3B_1$ state is presumed to occur in the same region. There has been no direct observation of other glyoxal excited states, though a simple molecular orbital picture suggests a total of 32 n → π^* and $\pi \rightarrow \pi^*$ states.

In addition to their spectroscopic interest, the excited states of glyoxal are important photochemically. Glyoxal has been found to photodissociate into hydrogen, carbon monoxide, formaldehyde, and CHO radicals.[10-14] And the dissociation product yields have been related to individual

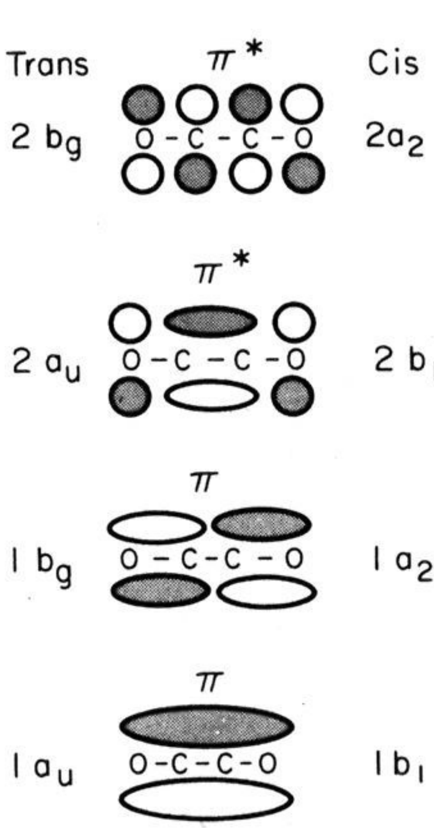

Figure 1. Qualitative representation of glyoxal π and π^* molecular orbitals. Shading represents the phase difference between lobes.

Table I. *trans*-Glyoxal Excited States[a]

Excitation	Open shell MO's	State symmetry	Triplet energy	Singlet energy
Ground state		^1A_g		−226.5182
$n \rightarrow \pi^*$	$7a_g\ 2a_u$	$1\text{-}A_u$	−226.3940	−226.3741
$\pi \rightarrow \pi^*$	$1b_g\ 2a_u$	$1\text{-}B_u$	−226.3680	−226.1762
$n \rightarrow \pi^*$	$6b_u\ 2a_u$	$1\text{-}B_g$	−226.3231	−226.3074
$\pi \rightarrow \pi^*$	$1a_u\ 2a_u$	$1\text{-}A_g$	−226.2480	−226.2450
$n \rightarrow \pi^*$	$7a_g\ 2b_g$	$2\text{-}B_g$	−226.2224	−226.2114
$\pi \rightarrow \pi^*$	$1b_g\ 2b_g$	$2\text{-}A_g$	−226.1511	−226.1474
$n \rightarrow \pi^*$	$6b_u\ 2b_g$	$2\text{-}A_u$	−226.1495	−226.1385
$n \rightarrow \sigma^*$	$7a_g\ 7b_u$	$2\text{-}B_u$	−226.1082	−226.0904
$\pi \rightarrow \pi^*$	$1a_u\ 2b_g$	$3\text{-}B_u$	−226.0814	−225.9734
$n \rightarrow \sigma^*$	$7a_g\ 8a_g$	$3\text{-}A_g$	−226.0188	−226.0072

[a] Each excited occupancy produces a singlet and triplet state of the given symmetry type. Arbitrary numerical prefixes distinguish states of the same symmetry. Energies correspond to vertical excitation and are in atomic units.

electronic states.[14-16] The reactive chemistry of carbonyl molecules also depends on the nature of the excited states. For instance, Yardley has proposed the existence of either a biradical intermediate or a charge-transfer complex between ^3A_u *trans*-glyoxal and olefins.[17]

Finding additional excited states by direct absorption spectroscopy appears limited because transitions from the ground state to some of the possible low-lying states are dipole forbidden. Specifically, these are the A_g and B_g states of *trans*-glyoxal and the A_2 states of *cis*-glyoxal. Also, higher energy states may be more difficult to identify because of the observed increasing diffuseness in the spectrum at shorter wavelengths.[3a] Recently, a ^1B_g state of glyoxal has been tentatively identified at about 30 000 cm^{-1} above the ground state, with the forbidden transition presumably induced by interaction with the solvent in a matrix.[18] In biacetyl, $CH_3COCOCH_3$, the observed change from small molecule to statistical or large molecule behavior in radiationless relaxation has been attributed to a ^3B_g state occurring energetically near the ^3A_u state.[19] This may support the possibility of a low-lying singlet–triplet pair of B_g states in glyoxal.

With only three excited states of glyoxal clearly identified and potential difficulties in extending experimental excited state information, theoretical considerations are appropriate. Theoretical methods may be useful in predicting the ordering of excited states and in providing some basis to support indirect experimental state identifications. And, in fact, several semiempirical studies have considered glyoxal and dicarbonyl excited states.[20-24] Both Hug and coworkers[20] and McGlynn and coworkers,[21] using CNDO calculations, indicate that of the $n \rightarrow \pi^*$ excitations, the lowest two should be $a_g \rightarrow a_u$ for trans and $a_1 \rightarrow b_2$ for cis followed by $a_g \rightarrow b_g$ and $a_1 \rightarrow a_2$. For both cis and trans, the separations between the two excitations were found to be about 1 eV in both calculations. In the more conventional notation used here, b_2 and b_1 representations are necessarily interchanged compared with the usage of Hug and McGlynn. This gives a B_1 state for their $a_1 \rightarrow b_2$ (now $a_1 \rightarrow b_1$) excitation, as observed.

Unfortunately, only Kato and coworkers considered $\pi \rightarrow \pi^*$ states in addition to $n \rightarrow \pi^*$ states.[24] Their results are in agreement with the ordering of $n \rightarrow \pi^*$ excitations, but in addition, they show a $\pi \rightarrow \pi^*$ ^3B_u state occurring between ^3A_u and ^3B_g $n \rightarrow \pi^*$ states. Furthermore, the ordering of ground state n and π orbitals is somewhat unexpectedly close. Ab initio calculations on the ground state[25-27] have been in reasonable agreement with this ordering of the valence molecular orbitals (MO's). And as already pointed out,[27] this suggests $\pi \rightarrow \pi^*$ excitations could be among low-lying states. As yet, no ab initio calculations of glyoxal excited states have been reported.

Theoretical Approach

Used in the calculations was a double ζ basis set of Dunning-contracted Gaussian functions,[28] C(9s 5p/4s 2p), O(9s 5p/4s 2p), and H(4s/2s). In calculations on the ground state of glyoxal,[27] this basis set has compared favorably with those used in other ab initio calculations.[25,26,29,30] A detailed review of basis sets has been presented elsewhere.[31]

In the previous calculation on the ground state,[27] the closed shell occupancies were confirmed to be

$$\ldots 5b_u^2\, 6a_g^2\, 1a_u^2\, 6b_u^2\, 1b_g^2\, 7a_g^2$$

for the trans form (C_{2h} symmetry) and

$$\ldots 6a_1^2\, 5b_2^2\, 1b_1^2\, 6b_2^2\, 1a_2^2\, 7a_1^2$$

for the cis form (C_{2v} symmetry). The π out-of-plane orbitals transform as a_u and b_g for trans and a_2 and b_1 for cis. The n or oxygen nonbonding orbitals are the highest filled a_g, b_u, a_1, and b_2 MO's. A pictorial representation of the π and π^* MO's is given in Figure 1. The orbitals are ordered by increasing number of nodes. While the representation may suggest a possible ordering of excited states, calculations were performed for all possible $n \rightarrow \pi^*$ and $\pi \rightarrow \pi^*$ excitations because of the close spacing of n and π ground state MO's.

Excited state occupancies were made by promoting one electron from each n and π orbital to an unfilled orbital. As shown in Tables I and II, for both cis and trans forms, there are ten such occupancies, arising from all $n \rightarrow \pi^*$ and $\pi \rightarrow \pi^*$ and two $n \rightarrow \sigma^*$ excitations. Each occupancy, of course, can produce a singlet and triplet state for a total of 40 states. Single configuration self-consistent-field (SCF) calculations were performed for these 40 states. Arbitrary numerical prefixes have been assigned to distinguish states of the same symmetry. Of course, only for the lowest state of each symmetry are the present calculations truly variational. The vertical excitation energy was calculated for all states. This is the energy of a given state at the geometry which is optimum for the cis or trans ground state.[27] Excited state calculations were performed only for the planar forms of the molecule. For gauche forms, the symmetry is reduced to C_2, for which only A and B states are defined,

Table II. *cis*-Glyoxal Excited States[a]

Excitation	Open shell MO's	State symmetry	Triplet Energy	Triplet Dipole moment	Singlet Energy	Singlet Dipole moment
Ground state		$^1A_1$			−226.5088	4.79
$n \rightarrow \pi^*$	$7a_1$ $2b_1$	1-B_1	−226.3899	4.76	−226.3705	4.80
$\pi \rightarrow \pi^*$	$1a_2$ $2b_1$	1-B_2	−226.3628	3.04	−226.1856	5.13
$n \rightarrow \pi^*$	$7a_1$ $2a_2$	1-A_2	−226.3314	4.12	−226.3164	4.32
$\pi \rightarrow \pi^*$	$1b_1$ $2b_1$	1-A_1	−226.2468	4.52	−226.2430	4.53
$n \rightarrow \pi^*$	$6b_2$ $2b_1$	2-A_2	−226.2086	4.29	−226.1971	4.28
$n \rightarrow \pi^*$	$6b_2$ $2a_2$	2-B_1	−226.1474	3.64	−226.1365	3.67
$\pi \rightarrow \pi^*$	$1a_2$ $2a_2$	2-A_1	−226.1420	2.92	−226.1382	2.91
$n \rightarrow \sigma^*$	$7a_1$ $7b_2$	2-B_2	−226.0888	1.07	−226.0669	0.73
$n \rightarrow \sigma^*$	$7a_1$ $8a_1$	3-A_1	−226.0812	3.08	−226.0699	2.86
$\pi \rightarrow \pi^*$	$1b_1$ $2a_2$	3-B_2	−226.0705	3.78	−225.9613	4.75

[a] Vertical excitation energies are in atomic units, and dipole moments in debyes.

and there is no longer a unique correspondence between orbital occupancies and electronic states. Hence, the simplest reasonable ab initio description of many of the analogous gauche electronic states of glyoxal would require configuration interaction.

With the interest of comparing SCF results with experiment, a partial geometry optimization was performed for the observed states. Comparison of these optimized results with experiment may enable one to precisely predict the energies of unobserved states. From ground state results, it was expected that carbon-hydrogen bond length and CCH angle optimization would not improve the energy as much as optimizing the carbon-carbon and carbon-oxygen bond lengths and perhaps the CCO angle. For ^3A_u, ^1A_u, $^3B_1$, and $^1B_1$, these last three structural parameters were quite nearly optimized by a simple parabolic fit of energy to parameter value, fitting one parameter at a time. The changes in energy for the CCO angle were small and so, only the C-C and C-O bond lengths were optimized in the two lowest unobserved states, ^3B_u and $^3B_2$.

Results and Discussion

The calculated energies of the forty excited states at geometries corresponding to the cis or trans ground state optimum strucutres are given in Tables I and II, and represented in Figure 2. The lowest vertical excited states are the observed 1-A_u ($n \rightarrow \pi^*$) and 1-B_1 ($n \rightarrow \pi^*$) states, though their energies relative to the ground state are higher than experimentally determined. Next are the trans 1-^3B_u and cis 1-$^3B_2$ states, both $\pi \rightarrow \pi^*$ excitations, and then another set of $n \rightarrow \pi^*$ states, 1-B_g and 1-A_2. Transitions to the ^1B_g state from the trans ground state and to the $^1A_2$ state from the cis ground state are dipole forbidden. The positions of states lying above around 60 000 cm^{-1} should be treated skeptically since Rydberg states (not treated here) become important in that region. The $n \rightarrow \sigma^*$ states were quite high in energy and need not be considered in discussions of the low-lying electronic states of glyoxal.

For all occupancies, the triplet state is lower in energy than the singlet and for most, the singlet and triplet are fairly close. The exceptions are the two B_u ($\pi \rightarrow \pi^*$) trans excitations and the two B_2 ($\pi \rightarrow \pi^*$) cis excitations. For these, the singlets were as much as 40 000 cm^{-1} higher than the corresponding triplets. These large singlet-triplet separations may be in part an artifact of the chosen basis set, which did not include diffuse or Rydberg-type functions. For an increasing number of $\pi \rightarrow \pi^*$ singlet states, it is now becoming clear that a purely valence-like description of the electronic structure is inadequate.[32-34] However, several test calculations using diffuse $p\pi$ functions lowered the total energies of these $\pi \rightarrow \pi^*$ singlet states by less than 0.01 hartree.

The geometry optimization gave rather minor changes for the $n \rightarrow \pi^*$ states, but substantially lowered the ^3B_u and $^3B_2$ states. The results are shown in Table III. The promotion of an electron to the lowest π^* MO, with a node between carbon and oxygen, produced a lengthening in the C-O separation for ^3A_u, ^1A_u, $^3B_1$, and $^1B_1$. Also, the carbon-carbon distances were slightly shortened for these states. The CCO bond angle changed little for the trans singlet and triplet but did increase in the cis states. For ^3B_u and $^3B_2$, an electron is excited from a π MO with no nodes to the lowest π^* MO. In the ground state, the filled π MO is energetically just above the second highest occupied n orbital (see ref 27). At vertical excitation, the ^3B_u and $^3B_2$, as expected, lie above the ^3A_u and $^3B_1$, respectively. But at the equilibrium geometry for the ^3B_u and $^3B_2$ states, the carbon-carbon bond length is contracted by about 0.15 Å and the carbon-oxygen bond length is about 0.15 Å longer than in the ground state. Their energies now become lower than any other excited state.

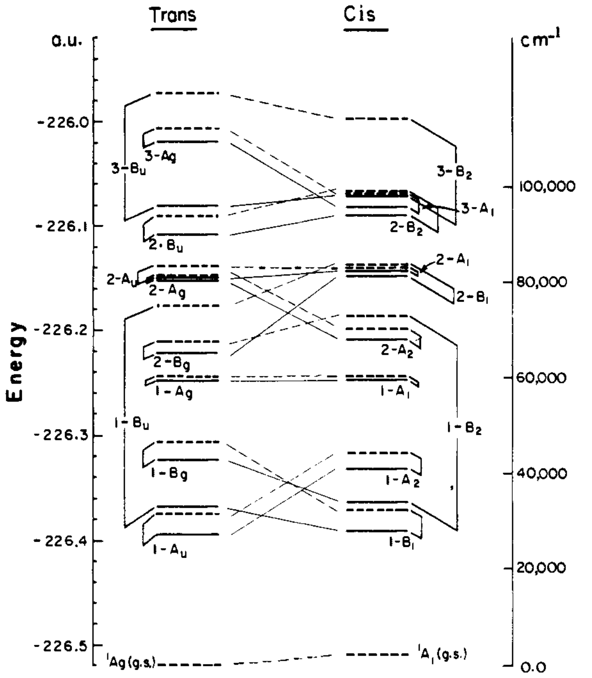

Figure 2. The excited states of glyoxal. Energies correspond to vertical excitation from the cis or trans ground state. Triplet states are shown with solid lines and singlet states with broken lines. Symmetry state designations are given for each singlet–triplet pair of states and correspond to excitations given in Tables I and II. Correlation lines between cis and trans states connect states which must correlate on the basis of symmetry, but do not represent any internal rotation potentials.

The calculated dipole moments of the cis states are given in Table IV. The dipole moment of the lowest $n \rightarrow \pi^*$ B_1 singlet and triplet is about the same as the ground state. For

Table III. Optimized Excited States[a]

	State	R_{CC}	R_{CO}	∠CCO	Energy, au	Energy relative to gs, cm^{-1}
Trans	^1A_g gs	1.508	1.215	121.1	−226.5182	0.0
	1^3A_u	1.492	1.241	121.0	−226.3959	26 850
	1^1A_u	1.494	1.244	121.7	−226.3766	31 090
	1^3B_u	1.353	1.356	121.1[b]	−226.4504	14 890
Cis	$^1A_1$ gs	1.516	1.213	123.2	−226.5088	0.0
	1^3B_1	1.492	1.236	124.7	−226.3921	25 620
	1^1B_1	1.494	1.241	125.1	−226.3733	29 740
	1^3B_2	1.350	1.356	123.2	−226.4480	13 340

[a] The carbon–carbon bond length, carbon–oxygen bond length, and carbon–carbon–oxygen angle were optimized for the lowest excited states. Bond lengths are in Å and angles are in degrees. [b] Not optimized; ground state (gs) value assumed.

Table IV. Mulliken Analysis of the $1b_1$ and $2b_1$ Orbitals of Glyoxal, for the $^3B_2$ and $^1B_2$ Excited Electronic State

Atom	$^3B_2$ state	$^1B_2$ state
	$1b_1$ Orbital	
O	0.39	1.79
C	1.61	0.26
	$2b_1$ Orbital	
O	0.79	0.07
C	0.21	0.93
	Total b_1 Orbital Populations	
O	1.18	1.81
C	1.82	1.19
	Total Atomic Populations	
O	8.13	8.31
C	6.06	5.89
H	0.81	0.80

most excitations, the singlet and triplet have nearly equal dipoles. The exceptions are the 1-B_2 ($\pi \rightarrow \pi^*$) and 3-B_2 ($\pi \rightarrow \pi^*$). Not surprisingly, these are the same excitations which gave the large singlet–triplet separations.

Prediction of States. Several factors must be considered when predicting electronic excitation energies T_e on the basis of SCF calculations. Aside from the quality of the chosen basis set, one must estimate effects of geometry optimization, correlation energy, and differences in vibrational zeropoint energies between states. The partial geometry optimization of the ^3A_u, ^1A_u, and $^1B_1$ states and the complete optimization of the cis and trans ground states[27] can be used to estimate some of the unknown effects. The partially optimized singlet states are about 9000 cm^{-1} above experimental 0-0 excitation energies. The ^3A_u state is also about 30% higher in energy than experimentally found. A more complete geometry optimization and possible differences in zeropoint energies could probably account for no more than 1000 cm^{-1} of the discrepancy.

The remaining errors are due either incompleteness of the basis set or correlation effects. In light of this, it is interesting to note a recent Hartree-Fock (i.e., large basis set) study of the n → π^* singlet and triplet states of formaldehyde.[35] There Garrison et al. found the SCF excitation energies to lie ~8000 cm^{-1} *below* experimental values. This would at first suggest that the glyoxal excitation energies are too high because of the basis set. To test this, vertical excitation energies were calculated for formaldehyde using the same basis set as with glyoxal. The geometry used was the experimentally determined ground state structure.[3a]

The results of these calculations, shown in Table V, agree with the larger basis set study[35] in finding the n → π^* energies too low. This suggests that the excitation energy errors introduced by our double ζ basis may be quite small for gloyoxal. However, this in turn implies that the true Hartree–Fock excitation energies in glyoxal are too ***high***, whereas in formaldehyde the opposite is the case. This result cautions us against models in which glyoxal is thought of as a superposition of two formaldehyde molecules. Interestingly, an analogous model has been successfully used by Dunning, Hosteny, and Shavitt[33] to discuss the electronic states of butadiene in terms of those of two ethylene units.

Table V. Formaldehyde Electronic States[a,b]

Excitation	State	Energy, au	Excitation energy, cm^{-1}
Ground state	$^1A_1$	−113.8295	0.0
n → π^*	$^3A_2$	−113.7426	19 100
	$^1A_2$	−113.7286	22 100
$\pi \rightarrow \pi^{*\prime}$	$^3A_1$	−113.6738	34 200
	$^1A_1$	−113.6674	35 600
$\sigma \rightarrow \pi^*$	$^3B_1$	−113.5737	56 200
	$^1B_1$	−113.5401	63 500
n → σ^*	$^3B_2$	−113.4909	74 300
	$^1B_2$	−113.4732	78 200

[a] Calculations were done with the same basis set as that used for glyoxal. Energies correspond to vertical excitation at the experimentally determined geometry[3a] of the ground state. [b] Note that the $\pi \rightarrow \pi^*$ $^1A_1$ state calculated does not correspond to physical reality, as it has a large Hamiltonian matrix element with the $^1A_1$ ground state of formaldehyde. CI calculations place this state much higher. See, e.g., S. D. Peyerimhoff and R. G. Buenker, "Chemical Spectroscopy and Photochemistry in the Vacuum-Ultraviolet", Reidel, Dordrecht-Holland, 1975.

Our conclusion at the present time concerning correlation effects in glyoxal is that they are somewhat unpredictable and can result in errors as large as 9000 cm^{-1} in Hartree–Fock excitation energies. Should more experimental information become available, it would be possible to calibrate SCF results for related systems, e.g., acrolein, and thus make rather accurate semiempirical predictions.

We can now attempt to estimate the positions of the next set of n → π^* states. The four 1-B_g and 1-A_2 states were calculated to have vertical excitation energies greater than 40 000 cm^{-1}. The π^* MO for these and the lower pairs of states is the same. Since the n orbitals are largely noninteracting, we expect the same geometry changes, correlation effects, and SCF error as with excitation from the other n orbital. Therefore, we estimate that the 1-^3B_g state occurs about 29 000 to 35 000 cm^{-1} above the ground state, with the 1-$^3A_2$ perhaps slightly lower. In correcting the singlet state energies, it is possible that the singlet–triplet separation should be larger than calculated. However, cis excitations which gave particularly large singlet–triplet separations had substantially different dipoles. We consider the reasons for this later, but at this point, we note the agreement in dipole moments of the 1-$^3A_2$ and 1-$^1A_2$ states. Then, the similarity of these states and the analogous trans states with the lower observed n → π^* states places the singlets above the triplets at an energy which can be taken as the experimental ^1A_u − ^3A_u difference, roughly 3000 cm^{-1}. This could support the recent experimental identification[18] of a ^1B_g state.

Perhaps the most careful estimate is required for the two low-lying $\pi \rightarrow \pi^*$ triplets. Once again, we expect that further geometry optimization would not significantly change the energies of the 1-^3B_u and 1-$^3B_2$ states. Lacking a configuration interaction calculation, correlation effects are difficult to estimate reliably as discussed earlier. But the surprisingly low energies of these $\pi \rightarrow \pi^*$ states suggests that their correlation energies may be less than that of the glyoxal ground state. Thus, the ^3B_u may lie between 12 000 and 22 000 cm^{-1} above the ground state, after estimating the theoretical uncertainty. Similarly, the $^3B_2$ state might be found between 11 000 and 21 000 cm^{-1} above the cis ground state. While 21 000 and 22 000 cm^{-1} represent upper limits to the calculation uncertainty, spectroscopic studies[4-9] at energies as low as about 18 000 cm^{-1} do not indicate the presence of these states. Thus, it seems possible that these will the lowest excited states of glyoxal.

However, as the referee has pointed out, the $^1A_g \rightarrow {}^3B_u$ transition should have a very low oscillator strength. Also the Franck-Condon factors will favor absorption at frequencies corresponding to vertical excitation. Thus, the maximum absorption for $^1A_g \rightarrow {}^3B_u$ may very well occur at higher energies than $^1A_g \rightarrow {}^1A_u$, and thus be obscured. Also the weak transition strength will be spread over a great wavelength region if these calculations are correct. Thus the lack of an experimental observation of the ^3B_u state does not necessarily place this state relative to the ^1A_u state.

In the vertical excitation energies, a very substantial break is found between the states so far considered and the higher states. Since even a sizable downward correction would not place these among the low-lying states, no attempt has been made to predict the true energies of the higher states.

The ^1A_u and $^1B_1$ states demonstrate an internal consistency of the calculations. Spectroscopic results have placed the $^1B_1$ about 335 cm^{-1} below the ^1A_u state[4-8] using the determined value[8] for the ground state cis-trans separation of 1125 cm^{-1}. If, instead, the calculated separation[27] of about 2070 cm^{-1} is used, the $^1B_1$ state will be 600 cm^{-1} above the ^1A_u. And this compares well with a difference of 715 cm^{-1} in the partially optimized, calculated $^1B_1$ and ^1A_u state energies.

Electronic Structure. The underlying interest in ab initio calculations on dicarbonyls is to attempt to relate the electronic structure and hopefully chemical properties of the whole system to the simpler electronic structure of a carbonyl group. And this should be useful in understanding the chemistry of large carbonyl systems. In ground state calculations,[27] a comparison between carbon monoxide, (CO)$_2$, and glyoxal made possible a better interpretation of the ordering of n and π valence MO's. The excited states show an even more significant relationship.

Many excited states of carbon monoxide have been observed and studied experimentally.[3a,36] In an ab initio configuration interaction study of carbon monoxide, O'Neil and Schaefer found a dominant configuration for 11 bound states including the observed states.[37] Two occupancies were found to yield the eight experimentally observed states:

$$1\sigma^2\, 2\sigma^2\, 3\sigma^2\, 4\sigma^2\, 5\sigma^2\, 1\pi^3\, 2\pi \qquad (1)$$

$$1\sigma^2\, 2\sigma^2\, 3\sigma^2\, 4\sigma^2\, 5\sigma\, 1\pi^4\, 2\pi \qquad (2)$$

The states arising from occupancy 1 have a fairly small singlet-triplet separation.[36] But the $\tilde{a}\ {}^3\Pi$ state and $\tilde{A}\ {}^1\Pi$ state, which arise from occupancy 2, differ in energy by about 2 eV. This is suggestive of the 1-B$_u$, 3-B$_u$, 1-B$_2$, and 3-B$_2$ excitations in glyoxal.

The probable existence of a carbon monoxide dimer has been shown in theoretical calculations.[38-40] Potential curves have been obtained showing three bound states of (CO)$_2$ in a constrained linear ($D_{\infty h}$) arrangement, with the lowest state, $^3\Sigma_g^-$, being bound with respect to the lowest available dissociation limit. The occupancy which gives rise to these states is,

$$1\sigma_g^2\, 2\sigma_g^2\, 3\sigma_g^2\, 4\sigma_g^2\, 5\sigma_g^2\, 1\sigma_u^2\, 2\sigma_u^2\, 3\sigma_u^2\, 4\sigma_u^2\, 1\pi_g^4\, 1\pi_u^2\, 2\pi_u^2 \qquad (3)$$

This occupancy, however, does not correlate (for collinear geometries) with the ground state occupancies of two CO molecules. In fact, the interaction between ground state CO molecules is repulsive (except for the long-range attraction), both in a linear arrangement[38] and nonlinear approaches.[27] However, by going to pathways of sufficiently low symmetry, it appears[40] that the $^1\Delta_g$ state of (CO)$_2$ can dissociate readily to two ground state CO molecules. The lowest dissociation limit accessible to the $^3\Sigma_g^-$ state of (CO)$_2$ is $\tilde{X}\ {}^1\Sigma^+$ plus $\tilde{a}\ {}^3\Pi$. Finally, occupancy 3 of the dimer correlates, though not uniquely, with the 1-B$_u$ and 1-B$_2$ electron occupancies of glyoxal.

This three-way correlation of excited states and occupancies is also indicated by the structures of the CO, (CO)$_2$, and glyoxal states. Experimentally, the carbon monoxide bond length is about 0.1 Å longer in the $\tilde{a}\ {}^3\Pi$ state than in the ground state. Similarly, the C–O bond length is about 0.14 Å longer in the ^3B_u and $^3B_2$ states of glyoxal than in the gound state. The minimum in the C–C distance potential for CO dimer was found to be 1.335 Å.[38] For the analogous glyoxal states, we find the C–C distance to be 1.353 in the trans form and 1.350 Å in the cis form.

Correlation of additional states is much more difficult, since occupancy 1 of carbon monoxide has two open-shell π MO's. Such a correlation will not be unambiguous and can give doubly excited glyoxal states. The most important result of the discussion of CO, CO dimer, and glyoxal states is the rationalization of the low-lying ^3B_u and $^3B_2$ states. Specifically, an electronically excited CO monomer is required to form the ground state of (CO)$_2$ and in glyoxal, this state becomes a very low-lying $\pi \rightarrow \pi^*$ state.

Explanation of the anomalous singlet-triplet separation and dipole differences of the 1-B$_u$, 3-B$_u$, 1-B$_2$, and 3-B$_2$ excitation requires examination of the wave functions. Considering as an example the 1-B$_2$ states, we note that only a few orbitals provide different singlet-triplet contributions to the total dipole moment. For these orbitals, atomic Mulliken populations show remarkable differences between the singlet and triplet. In particular, as seen in Table IV, the 1b$_1$ and 2b$_1$ orbitals essentially "switch" character in going from the $^3B_2$ to the $^1B_2$ state. Since the 1b$_1$ orbital is doubly occupied, while the 2b$_1$ orbital is singly occupied, this change in character strongly affects the total atomic populations, as well as the dipole moments. Note that the doubly occupied 1b$_1$ orbital is of C$^-$O$^+$ character for the $^3B_2$ state, but C$^+$O$^-$ character for the $^1B_2$ state. Immediately, this accounts for the larger dipole moment of the singlet. The half-filled 1a$_2$ orbital is similar in both singlet and triplet. The large singlet-triplet separation is probably connected with the interchange in the nature of the 1b$_1$ and 2b$_1$ orbitals, but a CI description of the wave functions may be necessary to fully understand this connection. For the other $\pi \rightarrow \pi^*$ excitations, the arguments are analogous.

Of perhaps primary importance in this work is the nature of the predicted low-lying ^3B_u and $^3B_2$ states. We first point out that the localization of the b$_1$ MO's causes the states to be biradicals. This is consistent with the CO-dimer state, $^3\Sigma^-$, which has been described as a biradical[38] and which correlates with the glyoxal $\pi \rightarrow \pi^*$ triplets. It is worthwhile to note that the singlet states which arise from the same excitation are not biradicals because of the singlet-triplet 1b$_1$-2b$_1$ MO reversal in localization. The carbon-carbon bond of the ^3B_u and $^3B_2$ states is essentially a double bond, consistent with the bond length shortening, and thus the structures can be represented as

^3B_u

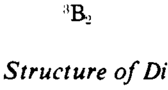

$^3B_2$

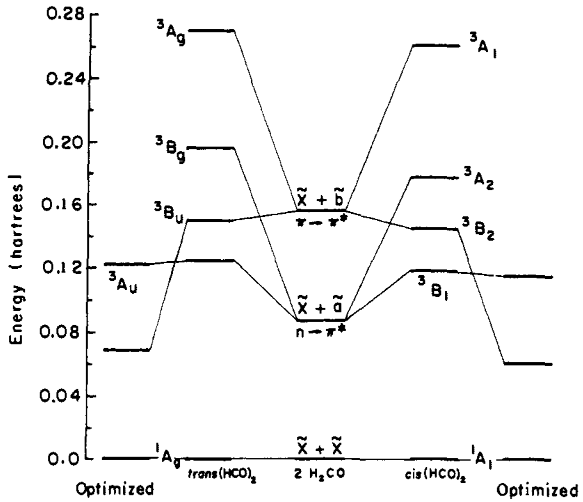

Figure 3. Correlation of the lowest triplet states of glyoxal with those of two formaldehyde molecules.

As with $^3\Sigma^-$ CO dimer, the high reactivity of a biradical could make the observation of these states difficult.

As mentioned earlier, another model in terms of which to discuss the electronic spectrum of glyoxal involves the superposition of two H_2CO molecules. This sort of "molecules in molecules" model has been successfully used to describe several excited electronic states of butadiene recently.[33] In the same spirit we present in Figure 3 a correlation of the lowest triplet states of glyoxal with the n → π* and π → π* states of formaldehyde. Note of course that this model applies only to geometries of glyoxal rather comparable to those of formaldehyde. And we see that at the ground state equilibrium geometry, the n → π* state of glyoxal is indeed the lowest excited state, as is the case for formaldehyde. However, changes upon excited state geometry optimization are so severe as to bring into question the validity of this simple model. In addition, Figure 3 shows that at the vertical geometry the lowest π → π* state falls below the second n → π* state. Thus one can reasonably conclude that the "coupling" of the two fragments is rather strong in glyoxal.

The final consideration of this work is the correlation of cis and trans excited states. The complicated pattern of vertical excitations in Figure 2 has several interesting features. After placing the 1-^3B_u and 1-$^3B_2$ states below the 1-A_u and 1-B_1 states, respectively, it can be seen that the A_u trans states correlate with higher energy A_2 cis states. Similarly B_1 states correlate with higher B_g states. This would indicate that population of the unobserved A_2 and B_2 states could probably be followed by isomerization. If there is little or no barrier to the isomerization, then the existence of these states might explain short-wavelength diffuseness in the glyoxal spectrum. At still higher energies, n → π*, π → π*, and n → σ* states are considerably mixed. There will be several avoided crossings and some n → π* states of one isomer will be found to correlate with π → π* states of the other isomer.

Acknowledgment. The Datacraft 6024/4 minicomputer is supported by the National Science Foundation under Grant GP-39317. We thank Professors Karl Freed, Edward Lee, C. Bradley Moore, and James Yardley for helpful comments. The support of the DuPont Corporation for one of us (C.E.D.) is appreciated.

References and Notes

(1) Work performed under the auspices of the U.S. Energy Research and Development Administration.
(2) Du Pont Graduate Fellow.
(3) (a) G. Herzberg, "Electronic Spectra of Polyatomic Molecules", Van Nostrand-Reinhold, New York, N.Y., 1966; "Spectra of Diatomic Molecules", Van Nostrand-Reinhold, New York, N.Y., 1950, (b) J. C. D. Brand, *Trans. Faraday Soc.*, **50**, 431 (1954); (c) H. L. McMurry, *J. Chem. Phys.*, **9**, 241 (1941).
(4) J. Paldus and D. A. Ramsay, *Can. J. Phys.*, **45**, 1389 (1967).
(5) F. W. Birss, J. M. Brown, A. R. H. Cole, A. Lofthus, S. L. N. G. Krishnamachari, G. A. Osborne, J. Paldus, D. A. Ramsay, and L. Watmann, *Can. J. Phys.* **48**, 1230 (1970).
(6) D. M. Agar, E. J. Bari, F. W. Birss, P. Borrell, P. C. Chen, G. N. Currie, A. J. McHugh, B. J. Orr, D. A. Ramsay, and J.-Y. Roncin, *Can. J. Phys.*, **49**, 323 (1971).
(7) W. Holzer and D. A. Ramsay, *Can. J. Phys.*, **48**, 1759 (1970).
(8) G. N. Currie and D. A. Ramsay, *Can. J. Phys.*, **49**, 317 (1971).
(9) D. A. Ramsay and C. Zauli, *Acta Phys. Acad. Sci. Hung.*, **35**, 79 (1974).
(10) F. H. Dorman and A. S. Buchanan, *Aust. J. Chem.*, **9**, 49 (1956).
(11) F. E. Blacet and R. W. Moulton, *J. Am. Chem. Soc.*, **63**, 868 (1941).
(12) R. G. W. Norrish and J. G. A. Griffiths, *J. Chem. Soc.*, 2829 (1928).
(13) J. G. Calvert and J. N. Pitts, Jr., "Photochemistry", Wiley, New York, N.Y., 1966, p 376.
(14) C. S. Parmenter, *J. Chem. Phys.*, **41**, 658 (1964).
(15) J. T. Yardley, *J. Chem. Phys.*, **56**, 6192 (1972).
(16) L. G. Anderson, C. S. Parmenter, and H. M. Poland, *Chem. Phys.*, 1, 401 (1973).
(17) J. T. Yardley, *J. Am. Chem. Soc.*, **94**, 7283 (1972).
(18) J. Kelder, H. Cerfontain, J. K. Eweg, and R. P. H. Rettschnick, *Chem. Phys. Lett.*, **26**, 491 (1974).
(19) E. Drent, R. P. van der Werf, and J. Kommandeur, *J. Chem. Phys.*, **59**, 2061 (1973).
(20) W. Hug, J. Kuhn, K. J. Seibold, H. Labhart, and G. Wagniere, *Helv. Chim. Acta*, **54**, 1451 (1971).
(21) J. F. Arnett, G. Newkome, W. L. Mattice, and S. P. McGlynn, *J. Am. Chem. Soc.*, **96**, 4385 (1974).
(22) J. R. Swenson and R. Hoffmann, *Helv. Chim. Acta*, **53**, 2331 (1970).
(23) E. Drent and J. Kommandeur, *Chem. Phys. Lett.*, **14**, 321 (1972).
(24) H. Kato, H. Konishi, H. Yamabe, and T. Yonezawa, *Bull. Chem. Soc. Jpn.*, **40**, 2761 (1967).
(25) U. Pincelli, B. Cadioli, and D. J. David, *J. Mol. Struct.* **9**, 173 (1971).
(26) T.-K. Ha, *J. Mol. Struct.*, **12**, 171 (1972).
(27) C. E. Dykstra and H. F. Schaefer, *J. Am. Chem. Soc.*, in press.
(28) T. H. Dunning, *J. Chem. Phys.*, **53**, 2823 (1970).
(29) L. Radom, W. A. Lathan, W. J. Hehre, and J. A. Pople, *Aust. J. Chem.*, **25**, 1601 (1972).
(30) K. R. Sundberg and L. M. Cheung, *Chem. Phys. Lett.*, **29**, 93 (1974).
(31) H. F. Schaefer, "The Electronic Structure of Atoms and Molecules: A Survey of Rigorous Quantum Mechanical Results", Addison-Wesley, Reading, Mass., 1972.
(32) C. F. Bender, T. H. Dunning, H. F. Schaefer, W. A. Goddard, and W. J. Hunt, *Chem. Phys. Lett.*, **15**, 171 (1972).
(33) T. H. Dunning, R. P. Hosteny, and I. Shavitt, *J. Am. Chem. Soc.*, **95**, 5067 (1973).
(34) P. J. Hay and I. Shavitt, *J. Chem. Phys.*, **60**, 2865 (1974).
(35) B. J. Garrison, H. F. Schaefer, and W. A. Lester, *J. Chem. Phys.*, **61**, 3039 (1974).
(36) P. H. Krupenie, *Natl. Stand. Ref. Data Ser., Natl. Bur. Stand.*, **No. 5** (1966).
(37) S. V. O'Neil and H. F. Schaefer, *J. Chem. Phys.*, **53**, 3394 (1970).
(38) N. H. F. Beebe and J. R. Sabin, *Chem. Phys. Lett.*, **24**, 389 (1974).
(39) J. Fleishhauer, M. Beckers, and H. D. Scharf, *Tetrahedron Lett.*, **43**, 4275 (1973).
(40) R. C. Haddon, D. Poppinger, and L. Radom, *J. Am. Chem. Soc.*, **97**, 1645 (1975).